HHS Public Access

Author manuscript

Chem Biol Interact. Author manuscript; available in PMC 2022 November 01.

Published in final edited form as:

Chem Biol Interact. 2021 November 01; 349: 109650. doi:10.1016/j.cbi.2021.109650.

The Thr45Gly substitution in yeast alcohol dehydrogenase substantially decreases catalysis, alters pH dependencies, and disrupts the proton relay system

Suresh Pal[1], **Bryce V. Plapp**[*]

Department of Biochemistry, The University of Iowa, Iowa City, IA 52246, USA

Abstract

X-Ray crystallography shows that the hydroxyl group of Thr-45 in the fermentative alcohol dehydrogenase (ADH1) from *Saccharomyces cerevisiae* is hydrogen-bonded to the hydroxyl group of the alcohol bound to the catalytic zinc and is part of a proton relay system linked to His-48. The contribution of Thr-45 to catalysis was studied with steady state kinetics of the enzyme with the T45G substitution. Affinities for coenzymes decrease by only 2–4-fold, but the turnover numbers (V/E_t) and catalytic efficiencies (V/K_mE_t) decrease 480-fold and 2900-fold for the oxidation of ethanol and 450-fold and 8400-fold for acetaldehyde reduction, respectively, relative to wild-type enzyme. Binding of NADH appears to require protonation of a group with a pK value of ~ 7.4 in wild-type ADH1, but the pK value for T45G ADH1 appears to be less than 5. For wild-type enzyme, the pH dependencies for ethanol oxidation (V_1/E_t and V_1/K_bE_t) are maximal above pK values of 7.0 to 7.7 and are attributed to the ionization of the alcohol or water bound to the catalytic zinc facilitated by His-48 in the enzyme-NAD^+ complexes. For T45G ADH1, these pK values are shifted to 6.3. The reduction of acetaldehyde (V_2/E_t and V_2/K_pE_t) modestly increases as the pH increases for wild-type and T45G enzymes. The removal of the hydroxyethyl group of Thr-45 disrupts the connection of the oxygen of ligands bound to the catalytic zinc with the proton relay system and formation of productive catalytic states. The conformational change of the enzyme and the exchange of ligands on the catalytic zinc can also be affected. Assignments of groups responsible for the pK values are discussed in the context of studies on other forms of horse liver and yeast ADHs. The substitutions with Ala-45 and Cys-45 in yeast ADH1 and the homologous substitutions with Ala-48 in horse and human liver ADHs also significantly decrease catalytic efficiency. Threonine or serine residues at this position in alcohol dehydrogenases are highly conserved and contribute substantially to catalysis.

[*]Corresponding author: Tel: +1 319-335-7909; fax: +1 319-335-9570; bv-plapp@uiowa.edu.

[1]Present address: 160 High Tides, Apt. 104, Columbus, OH 43235; Tel: 614-370-9747;

Authors' Contributions. **Dr. Suresh Pal**: Investigation, Formal analysis, First draft. **Prof. Bryce V. Plapp**: Conceptualization, Funding, Methodology, Investigation, Resources, Validation, Data curation, Visualization, Revisions.

Conflicts of interest

The authors declare that they have no known competing financial interests or personal relationships that could have appeared to influence the work reported in this paper.

Keywords

Enzyme mechanism; Enzyme kinetics; Mutagenesis; Protein structure; Proton transfer

1. Introduction

Alcohol dehydrogenases (EC 1.1.1.1) oxidize alcohols by catalyzing hydride transfer to NAD^+ and proton transfer to solvent. The first X-ray structure of horse liver ADH1E (ethanol-active isoenzyme) showed a hydrogen-bonded system connecting the zinc-bound water to Ser-48 and His-51, which could act as a base in the proton transfer [1, 2]. A structure of a ternary complex with NAD^+ and an alcohol shows that the full system includes the oxygen of the alcohol bound to the catalytic zinc, the hydroxyl group of Ser-48, the 2'-hydroxyl group of the nicotinamide ribose, and the imidazole group of His-51 as shown in Scheme 1 [3]. The hydrogens are implied by the three-dimensional structures, and the small shift of the hydrogens effectively relays a proton from the zinc ligand to water. The zinc-alkoxide is stabilized by a "low-barrier" hydrogen bond with the Ser-48 hydroxyl group at an O–O distance of 2.5 Å [4–7].

Studies of the pH dependence of catalysis of horse liver ADH1E suggest that a histidine residue participates in catalysis, but ionization of the water or alcohol bound to the zinc is also involved [8–11]. In the apoenzyme, a water replaces the 2'-hydroxyl group of the coenzyme and can maintain the connection between the water bound to the zinc and His-51 [12]. Substitution of His-51 with a glutamine residue significantly decreases the rate constants and alters the pH dependencies for binding of coenzymes and catalytic reactions, and X-ray crystallography shows that the glutamine can isosterically replace His-51 in binding [13, 14]. Oxidation of alcohols by yeast ADH1 is maximal above a pK value of ~7.6, consistent with a role for the homologous His-48 as a proton acceptor [15–21]. Diethyl pyrocarbonate decreases activity of both yeast and liver alcohol dehydrogenases, supporting a role for a histidine in catalysis [17, 22]. Substitution of His-48 in yeast ADH1 with glutamine or glutamic acid decreases catalytic efficiencies and alters the pH dependencies [23, 24].

Sequence and structural alignments show that Ser-48 in horse ADH1E is homologous to Thr-45 in yeast ADH1 and that serine or threonine at this position is conserved in alcohol dehydrogenases [25, 26]. Three-dimensional structures of yeast ADH1 confirm that the proton relay system with Thr-45 and His-48 is present [27–29]. The T45S substitution in yeast ADH1 has less than 2-fold effects on the kinetics [30], but substituting Thr-45 in yeast ADH1 with alanine or cysteine residues "inactivates" the enzyme [24]. The S48A substitution in horse ADH1E decreases catalytic efficiency by ~10^5-fold and binding of coenzymes by 4–40-fold [6]. The S48T substitution in horse ADH1E has small effects on the reaction with ethanol, but alters the stereoselectivity for oxidation of secondary alcohols [6]. Inspection of the horse and yeast ADH1 structures suggests that substituting the serine or threonine with alanine would disrupt the binding of the oxygens of substrates and coenzymes and block the proton transfer. A cysteine sulfhydryl group also might not fit well and transfer a proton. However, we thought that the T45G substitution in the yeast enzyme

might allow some catalytic activity because a water molecule might fit in the location of the hydroxyl group of Thr-45 and facilitate the interaction of the substrate oxygen between the catalytic zinc and the 2'-hydroxyl group of the nicotinamide ribose. Molecular models based on the X-ray structure of the complex of the yeast enzyme with NAD^+ and trifluoroethanol are shown in Fig. 1.

In this study, the kinetics and pH dependencies of catalysis for the T45G enzyme were determined and compared to results with horse liver and yeast ADHs. These enzymes have similar mechanisms. However, the catalytic zinc in the open conformation of the yeast apoenzyme has an "inverted" coordination to Cys-43, His-66, Glu-67 and Cys-153, and when coenzymes bind and the conformation closes, water or alcohol displaces Glu-67 to form the "classical" coordination [27–29]. In contrast, the coordination of the zinc in the liver apoenzyme and ternary complexes are both classical, but interchange of water and substrates bound to the zinc in complexes is required for catalysis [5, 12]. The differences in zinc coordination of the yeast and liver apoenzymes apparently cause significant changes in the pH dependence of coenzyme binding.

2. Experimental Procedures

2.1. Site-directed mutagenesis

The single stranded template in M13mp18RF phage derived from the gene for yeast ADH1 (*adc1*, YOL086c, UniProtKB entry P00330) in the yeast shuttle vector YEp13 [32, 33] was mutated with the oligonucleotide primer TCTGTCACGGTGACTTGCA (underline marks the site of mutation) by standard methods [34–36]. The mutation was confirmed by sequencing the singe-stranded M13 phage [37]. The T45A and T45C substitutions described previously were also confirmed by peptide mapping and amino acid sequencing [21, 36]. The fragment generated by *Sph* I restriction was subcloned into the yeast shuttle vector YEp13 and transfected into *E. coli* XL1-Blue cells for preparation of the plasmid, which was then transfected into an ADH-negative strain of *S. cerevisiae* for production of the substituted ADH [38, 39].

2.2. Enzyme purification

Yeast were grown to full density (OD_{600} = 12 cm^{-1}) at 30 °C in 6 1.5-L flasks of YPD medium (1% yeast extract, 2% peptone, 2% glucose), with vigorous shaking so that the yeast did not require fermentation to grow. The enzyme was purified by precipitation with protamine sulfate and PEG4000 and chromatography on DEAE-Sepharose CL-6B and Octyl-Sepharose CL-4B [21, 39]. The final enzyme preparation appeared to be free of other proteins by SDS and native polyacrylamide gel electrophoresis. The concentration of purified protein was estimated using A_{280} = 1.26 cm^{-1} $(mg/ml)^{-1}$. From ~69 g of cells, ~80 mg of purified T45G enzyme was obtained. The concentration of active sites was determined by spectrophotometric titration with NAD^+ in the presence of 10 mM pyrazole [40]. Enzyme activity was determined in a standard assay and used to control enzyme concentrations for the kinetics experiments [41].

2.3. Steady-state kinetics

Ethanol and acetaldehyde were redistilled before use. NAD^+ and NADH were purchased from Boehringer Mannheim Biochemical Co. Ethanol-d_6 was from MSD Isotopes.

A buffer designed to mimic physiological conditions of 83 mM potassium phosphate, 40 mM KCl and 0.25 mM EDTA, pH 7.3, was used at 30 °C for the kinetics experiments [42]. Enzyme activity was determined by measuring the change in absorbance at 340 nm with a spectrophotometer connected to a computer with a FORTRAN program to estimate initial velocities with a linear or parabolic fit of the data. The kinetic constants for the sequential bi mechanism were determined by initial velocity studies with concentrations of both substrates varied over a 17-fold range in a systematic manner (5 × 5 matrix, with duplicate assays) and fitting the data to the kinetic equation ($v = V_1[A][B]/(K_{ia}K_b + K_a[B] + K_b[A] + 1)$) for the sequential bi reaction with the SEQUEN program, where concentrations of reactants (A = NAD^+, B = alcohol) are given in brackets, and the kinetic constants for the respective substrates have the corresponding subscripts [43]. For the reverse reaction, P = aldehyde is substituted for B, and Q = NADH is substituted for A. Standard errors for kinetic constants were usually <10–15 % of the values, indicating good estimates.

The pH dependencies of kinetic constants were determined at 30 °C by initial velocity studies with substrate concentrations varied from 17.6 to 300 mM ethanol and 0.176 to 3.0 mM NAD^+ or for the reverse reaction usually with 6 to 100 mM acetaldehyde and 6 to 100 μM NADH (or 2-fold lower at low pH and 2–4-fold higher at high pH) in a 5 × 5 matrix of concentrations with duplicate assays. Buffers of 10 mM sodium pyrophosphate ($Na_4P_2O_7$) and 0.25 mM EDTA containing sufficient H_3PO_4, NaH_2PO_4 and Na_2HPO_4 to produce a final ionic strength of 0.1 and the desired pH were used [21]. The buffers in the pH range of 5.5 to 9.0 were prepared by mixing stock solutions with pH of 5.5 and 9.5 in the appropriate ratios. The buffers with pH over 9.0 were prepared from stock solutions of pH 9.4 and 10.7 that contained 10 mM sodium pyrophosphate, 0.25 mM EDTA, and 5 mM sodium carbonate for good buffering capacity. All buffers were made as double strength and diluted in the reaction mixture with substrates just before the assays were started. The pH did not change significantly after the enzyme reaction. The pK values for the pH dependencies were determined by fitting the kinetic constants with a nonlinear least-squares program (NONLIN, C. M. Metzler, The Upjohn Co.) to equations derived for various mechanisms.

3. Results

3.1. T45G enzyme properties

The enzyme was purified in good yield by the same procedure as for wild-type enzyme, but the T45G enzyme had greatly reduced enzyme activity. The A_{280}/A_{260} ratio was 1.68 (similar to wild-type enzyme), suggesting that endogenous nucleotide was not bound to the protein. The titration with NAD^+ in the presence of 10 mM pyrazole showed the same difference absorption peaks at 283 and 292 nm as for wild-type enzyme, and the apparent K_d for NAD^+ was about the same as for wild-type enzyme. The T45G substitution does not appear to affect the interaction of the pyrazole with the catalytic zinc or the formation of the partial covalent bond with the nicotinamide ring, which has been observed with the horse

liver enzyme [44]. Based on the protein concentration determined from the absorption at 280 nm and the titration of active sites, 65 % of the subunits could bind NAD^+, typical of many preparations of the yeast enzyme.

3.2. T45G enzyme kinetic constants and mechanism

The kinetics of oxidation of ethanol and reduction of acetaldehyde show intersecting initial velocity patterns, consistent with the sequential bi bi mechanism typically found for ADHs. The kinetic constants in Table 1 show that the magnitudes of all of the constants change as a result of the T45G substitution. The equilibrium constant calculated from the kinetic constants agrees fairly well with the established value, suggesting that the constants are internally consistent. The inhibition constants for NAD^+ (K_{ia}) and NADH (K_{iq}) decrease about 2–4-fold, indicating that affinity for the coenzymes is not significantly affected. The K_b for ethanol and K_p for acetaldehyde increase 6-fold and 18-fold, respectively. The dissociation constant (K_i) for 2,2,2-trifluoroethanol, a competitive inhibitor of ethanol, increases 10-fold, indicating weaker interactions of the alcohol in the substrate binding pocket. The most drastic changes are the ~470-fold decreases in turnover numbers for oxidation of ethanol (V_1/E_t) and reduction of acetaldehyde (V_2/E_t), and the overall decreases of 2900–8400-fold in catalytic efficiencies (V_1/K_bE_t and V_2/K_pE_t).

The kinetic mechanism of wild type yeast ADH1 is preferentially ordered, with coenzymes binding before the other substrates, and release of product coenzyme is partially rate-limiting for turnover [20, 39, 46–48]). The large decreases in turnover numbers for the T45G enzyme could indicate that hydrogen transfer has become rate-limiting, which would be expressed as larger isotope effects when oxidation of deuterated ethanol and protio-ethanol are compared. The results in Table 2 show that the deuterium isotope effects increase somewhat because of the T45G substitution. The effects are consistent with a more random mechanism, with partial rate-limitation by hydride transfer, but still with a preferred order with coenzyme binding first because $^D V_1/K_bE_t$ is somewhat larger than $^D V_1/K_aE_t$. Similar studies with other mutated forms of yeast ADH also show somewhat elevated isotope effects [30]. Nevertheless, hydride transfer has not become fully rate-limiting because the intrinsic isotope effect is about 6 [19, 20], and it appears that isomerization of some complexes in the mechanism are also partially rate-limiting [36]. X-ray crystallography and cryogenic electron microscopy show that the protein changes conformation when coenzymes bind, and the coordination of the catalytic zinc inverts when substrates are bound [27–29].

3.3. pH Dependencies of reactions catalyzed by the T45G enzyme

The pH dependencies of the kinetic constants provide insight into the catalytic mechanism, although it can be difficult to assign which of the many groups on the enzyme contribute to a pH dependence [50]. The kinetic constants were determined as a function of pH for both the forward and reverse reactions (Table 3). The same buffer system was used previously for the wild-type and various substituted enzyme forms [21, 36]. The data in Table 3 show significant pH dependencies.

The pH dependencies are illustrated in Fig. 2 and were analyzed by fitting the relevant kinetic parameters with logarithmic functions. The parameters that fit the data are

summarized in Table 4 and compared to the values for the wild-type enzyme. Because the kinetic constants are comprised of multiple microscopic rate constants, the pK values are apparent and can be shifted from true values by commitment factors in the enzymatic mechanism [20, 51]. The pH dependencies for wild-type and H44R enzymes were determined previously [21]. The remarkable results are that the pH dependencies have been significantly altered by the T45G substitution, which does not change an ionizable group. The oxidation of ethanol (V_1/E_t and V_1/K_bE_t) is described by a simple function where the rate constant is maximal at high pH when some group with a pK of ~6.3 becomes deprotonated. In contrast, the pH dependence for wild-type enzyme shows a wave function where the enzyme is somewhat more active at high pH than at low pH and described by ionization of some group with a pK of 7.0 or 7.7. The kinetic constant V_1/E_t includes rate constants for all of the steps in the mechanism after formation of the ternary complex (including release of products and any isomerizations), whereas the kinetic constant V_1/K_bE_t includes the binding of ethanol, hydride transfer, release of acetaldehyde, and any isomerizations, and thus its pH dependence is more related to the chemical step in the mechanism. The binding of NAD^+ ($1/K_{ia}$) for wild-type enzyme shows somewhat tighter binding at low pH than at high pH, and the binding by the T45G enzyme is similar but with an almost linear dependence. The apparent rate constants for association of NAD^+ (V_1/K_aE_t) for wild-type and T45G enzymes do not exhibit definitive pH dependencies.

For the reverse reaction catalyzed by the T45G ADH, V_2/E_t and V_2/K_pE_t show a small, but linear, increase as pH decreases, whereas the wild-type enzyme has somewhat higher activity at low pH than at high pH that can be fitted by pK values of 7.0 or 7.8, for some groups on the enzyme that modulate activity. The pH dependencies of wild-type enzyme for V_2/K_qE_t, which is related to the rate constant for association of NADH to the enzyme, and $1/K_{iq}$, which is the binding constant for NADH, show that protonation of some group with a pK value of 7.8 or 7.4 increases the kinetic constant. In contrast, the pH dependencies for these parameters with the T45G enzyme are almost linear with a slope of about – 0.8, which can indicate that stoichiometric protonation of the enzyme facilitates binding of NADH. Binding of NAD^+ and NADH are controlled differently by these enzymes.

4. Discussion

4.1. Structural basis for understanding the effects of the T45G substitution

The recent structures of the wild-type yeast enzyme provide a framework of interpreting the effects of the T45G substitution on the kinetics and mechanism of the enzyme [27–29]. X-ray crystallography of two different forms of wild-type yeast ADH1 crystallized with NAD^+ and 2,2,2-trifluoroethanol shows that the tetrameric molecule (147396 Da) has back-to-back dimers where each dimer has one subunit in a closed conformation with NAD^+ and the catalytic zinc in the classical coordination with bound trifluoroethanol, and the other subunit has an open conformation with or without NAD^+, and the zinc has an inverted coordination (4W6Z.pdb, 5ENV.pdb). Each subunit has a coenzyme binding domain and a catalytic domain, and a rotation of ~12° closes up the substrate binding site. The conformational change appears to be coupled to the change in zinc coordination because Arg-340 interacts with coenzyme and Glu-67 moves from the zinc to interact with Arg-340

[29]. The coenzyme binding domains of two subunits interact about a molecular 2-fold axis with an extended β-sheet of the Rossmann fold. The asymmetry of the dimers in the crystal forms is apparently due to crystal lattice interactions because cryo-electron microscopy shows *D*2 symmetry for the tetramers (four identical subunits) for the open conformations of the apoenzyme (7KCQ.pdb) and one enzyme-NADH complex (7KJY.pdb) and for the closed conformations of another complex with NADH (7KC2.pdb) and a ternary complex with NAD^+ and trifluoroethanol (7KCB.pdb).

The subunit with the open conformation in crystals can bind and release NAD^+ even in the presence of trifluoroethanol, whereas NAD^+ does not dissociate from the subunit with the closed conformation. Thus, the conformational change strengthens the binding of NAD^+, but the energetics of the change with the yeast ADH are not known [28]. Binding of NAD^+ to the open conformation of the protonated horse liver enzyme has a K_d of 0.67 mM at pH 8 (similar to the value of 1.0 mM for the wild-type yeast enzyme [11]), and after deprotonation and the conformational change, the horse enzyme has an observed dissociation constant for NAD^+ of 27 μM [52]. The dissociation constants for NAD^+ or NADH with the yeast and liver enzymes differ in part because of different interactions with the adenine ring [53].

The overall mechanism is shown in Scheme 2, where E represents the open conformation of the enzyme forms with the inverted zinc coordination with Glu-67, and F represents the closed conformation with the classical zinc coordination with a water or substrate oxygen. There is structural evidence for the F-NAD^+ and F-NADH complexes with bound water [29]. The oxygens of the alcohol (Alc) or aldehyde (Ald) substrates replace the zinc-bound water, probably facilitated by the intermittent binding of Glu-67 [26, 28, 29]. It is also possible that the E-NAD^+ complex is directly converted to F-NAD^+-Alc by a concerted binding and conformational change, bypassing the F-NAD^+-water complex, especially at high concentrations of alcohol. The mechanism of horse liver ADH1 differs because the liver apoenzyme has the classical coordination of the zinc, and after coenzyme binds and the conformation closes, the exchange of alcohol or aldehyde for a water probably involves a transient inversion of the zinc coordination [11, 12].

In the ternary complex (Fig. 1), the proton relay system (Scheme 1) can facilitate deprotonation of the alcohol to form the alkoxide (Alk), which is oxidized to the aldehyde, or the protonation of the alkoxide for the reverse reaction. In this mechanism, the zinc-water or zinc-alcohol and His-48 in the proton relay system might have pK values in the range of 5.5 and 10, and the state of protonation could affect the catalytic activities of the wild-type or T45G enzymes. However, the T45G substitution might disrupt the proton relay or accommodate a water molecule that replaces the hydroxyl group of the threonine and still facilitates proton relay.

Several ionizable amino acid residues interact with the coenzyme and could contribute to catalysis and pH dependencies (Fig. 3). Lys-206 NZ binds to the adenosine ribose O3D. The imidazole ND1 of His-44 makes a hydrogen bond to the pyrophosphate O2A of the coenzyme. The 3'-hydroxyl group of the nicotinamide ribose donates a hydrogen bond to the imidazole NE2 of His-48, and ND1 of His-48 donates a hydrogen bond to the carboxyl

group of Asp-53. Other nearby residues include His-15 and His-51 in the opening to the active site, and His-138 near the interface between subunits. It appears that His-15 is not directly involved in catalysis because the H15R substitution changes the kinetic constants by less than 2-fold [54].

Ligands to the catalytic zinc could also affect pH dependencies (Fig. 4). His-66 NE2 binds to the catalytic zinc and ND2 binds to the carboxylate of Asp-46, which also binds a water molecule buried behind the catalytic zinc. Glu-67 binds the catalytic zinc in the open conformation and to Arg-340 in the closed conformation. Both Asp-46 and Glu-67 appear to be carboxylates in the closed conformations as implied by the hydrogen bonding interactions with waters and protein groups (4W6Z.pdb, subunits A and C). The electron densities around Asp-46 and Glu-67 in the open conformation are less definitive (4W6Z.pdb, subunits B and D). The sulfhydryl groups of cysteine residues 43 and 153 certainly bind as thiolates to the catalytic zinc in the classical coordination, with bond distances of 2.3–2.4 Å, but the distance from Cys-153 SG to the zinc is ~2.5 Å in the inverted coordination [27]. The microscopic pK value for an isolated cysteine thiol is ~9, but in enzyme active sites, the range can be from 3–11 [55]. It is interesting that the exchange of Co^{II} for Zn^{II} in yeast ADH is accomplished by dialysis in sodium acetate buffer at low pH (4.5–5.2), although it is not clear if the catalytic zinc was substituted in yeast ADH as it was under similar conditions for horse liver ADH [56–59]. Protonation of a cysteine thiolate bound to the zinc could facilitate change in coordination, metal exchange, or acid/base catalysis. The pK value could be ~5 for a cysteine bound to the zinc in yeast ADH.

4.2. Related studies on horse liver alcohol dehydrogenase

Horse liver ADH1E has Arg-47. His-51, and Lys-228, corresponding to His-44, His-48, and Lys-206 in the homologous yeast ADH1, and comparisons with versions of yeast ADH1 are relevant [25, 27]. (Residues numbers in some previous publications on the yeast enzyme used horse liver ADH1E numbers because the structural model at that time was based on the liver ADH1E.) Yeast ADH1 with the H44R substitution should resemble horse ADH1E [21]. Binding of NAD^+ to ADH1E is tighter at high pH (up to pH 10) and is controlled by a group with a pK value of ~9.2 in free enzyme that shifts to a pK value of ~7.3 in the enzyme-NAD^+ complex and is attributed to ionization of the water bound to the catalytic zinc to form zinc-hydroxide [8, 11, 60, 61]. A proton is released when NAD^+ binds, and the deprotonated enzyme changes conformation and binds ligands [11, 60]. The rate constants for association of NAD^+ show a bell-shaped dependency with pK values of ~6.9 and ~9.0 [60, 62]. Binding of NADH is tightest at low pH, below a pK value of ~9.2, attributed to the zinc-bound water, which apparently shifts to 11.2 in the enzyme-NADH complex [63]. Thus, a proton is taken up when NADH binds to the enzyme [60]. The pH dependencies for binding of NAD^+ and NADH were also determined in other studies [20, 64]. The pH dependence for binding NAD^+ is inverted as compared to binding of NADH probably because affinity for the positively-charged nicotinamide ring of NAD^+ is favored with a negatively-charged zinc-hydroxide whereas binding of the neutral ring in NADH is favored by a neutral zinc-water [61, 65].

Above pH 10, affinity for both NAD^+ and NADH decreases, which can be attributed to deprotonation of Lys-228 with a pK value of 10.4 [63, 66] and is supported by the observations that binding of NAD^+ to the enzymes with the K228R substitution or with acetimidylated lysines is pH independent above pH 8 while binding decreases at low pH below a pK of 6.3–6.7, probably due to the zinc-water and His-51 in the proton relay [13, 62].

The H51Q substitution significantly decreases the rate constants for binding NAD^+, hydride transfer and catalytic efficiency for alcohol oxidation (V_1/K_bE_t) at pH 8 as the apparent pK value for the pH dependence shifts up from ~6.7 in wild-type enzyme to ~8.1, consistent with a role for His-51 in facilitating proton transfer from the zinc-bound water and in controlling the conformational change [11, 13, 14]. Moreover, the doubly substituted H51Q:K228R enzyme shows a pH dependence for association of NAD^+ and V_1/K_bE_t with pK values of ~9.0, which are assigned to the zinc-water. Structures of the H51Q:K228R ADH complexed with NAD^+ and fluorobenzyl alcohols determined at 1.8 Å show that the amino acid substitutions are accommodated with only small, local changes and that Gln-51 interacts with the 2'-hydroxyl group of the nicotinamide ribose [14]. The binding of NADH to the wild-type, H51Q, K228R, and H51Q:K228R ADHs is most rapid at low pH, decreasing at high pH above a pK value of ~9.6, probably related to ionization of the zinc-water [13].

4.3. The T45G substitution in yeast ADH differentially affects kinetic constants

The T45G substitution has small effects on the affinity for the coenzymes, even though the structural studies show that the hydroxyl group of Thr-45 interacts directly with the 2'-hydroxyl group of the nicotinamide ribose of the coenzyme. Perhaps the many other interactions of the coenzymes with the protein dominate the energetics, as adenine nucleotides bind well [67]. The K_i for trifluoroethanol binding increases 10-fold, suggesting that the hydrogen bonds to the Thr-45 hydroxyl group linking the oxygen of the alcohol bound to the zinc to the 2'-hydroxyl group of the NAD^+ are disrupted and cannot be fully replaced by a water molecule (Fig. 1).The most dramatic effect of the T45G substitution is the ~470-fold decrease in turnover numbers, which is also expressed in the catalytic efficiencies (V/K_mE_t) that reflect the binding of substrate, hydrogen transfer and release of the first product. The large effect could be due to binding of the substrate in less productive modes, interference with deprotonation of the alcohol or protonation of the alkoxide, or the isomerization that involves the change in zinc coordination. It does not appear that the zinc is locked in the inverted coordination with T45G ADH1 because UV spectroscopy shows that pyrazole forms the complex with the nicotinamide ring of NAD^+, as found in structures with horse liver ADH1 [44].

4.4. Interpretation of the pH dependencies for binding of coenzymes

The binding of NAD^+ to wild-type and T45G yeast ADHs is modestly tighter at low pH than at high pH and is fundamentally different (inverted) from the horse liver enzyme, which binds NAD^+ ~30-fold tighter at pH 9 than at pH 6, apparently controlled by ionization of the zinc-bound water in the apoenzyme [8, 60]. The pH dependence of the conformational change for the horse liver enzyme is most rapid at pH values below a pK value of 7.6

[11, 62]. The contrasting pH dependence can be because the zinc in the yeast apoenzyme is coordinated to the carboxylate group of Glu-67, and after coenzyme binds the enzyme changes conformation and a water binds to the zinc to produce F-NAD^+.

The ligand exchange is probably an “interchange” mechanism, with a transient trigonal bipyramidal, pentacoordinate intermediate [27, 68, 69], and might occur when a positively-charged nicotinamide ring and the thiolate of Cys-153 are nearby, and the hydroxyl group of Thr-45 can interact with the water that binds to the zinc and displaces Glu-67. Structures for the open conformation of the wild-type yeast enzyme show the oxygen of trifluoroethanol interacting loosely with the catalytic zinc (Fig. 4). A water could replace the oxygen of trifluoroethanol and interact with the zinc in the open conformation of the apoenzyme.

The small decrease in affinity of wild-type yeast enzyme for NAD^+ above a pK value of 8–9 could be related to deprotonation of a histidine residue [15, 21], typically with a pK value between 5 and 8 [55]. The H44R yeast enzyme binds NAD^+ modestly tighter than wild-type enzyme does in the pH range of 6–8, and even better at pH values above a pK of 9.8, consistent with some contribution of His-44 and Lys-206 to binding [21]. The H48Q enzyme binds NAD^+ with about the same affinity and the small pH dependence as wild type enzyme, suggesting that His-48 does not contribute to the pH dependence of binding [70].

The wild-type horse liver and yeast enzymes bind NADH tighter ($1/K_{iq}$) at low pH than at high pH [15, 20, 60]. Wild-type yeast ADH exhibits a pK value of 7.4 for $1/K_{iq}$ and a pK value of 7.8 for the kinetic parameter V_2/K_qE_t, related to the rate constant for association of NADH to free enzyme in an ordered mechanism. These pH dependencies do not appear to be due to His-44 or His-48 because the wild type, H44R, and H48Q enzymes have similar pH dependencies with pK values in the range from 7.2–7.9 [21, 70]. As suggested for horse ADH1E, ionization of the zinc-water could destabilize binding.

The T45G enzyme has unusual linear dependencies for binding of NADH, with a slope of ~ −0.7 for the binding constant ($1/K_{iq}$) and a slope of ~ −0.9 for the apparent rate constant for association (V_2/K_qE_t). It is as if a group with a pK below ~5 must be protonated for NADH to bind. (In Eq. 3, if K_1 is $\gg$ $[H^+]$, log k_{obs} has a linear dependence on pH.) In principle, such a pH dependence would exhibit a slope of −1.0 in the pH range from 6–9, but the activity coefficient for a hydronium ion in the environment of the enzyme could be altered. Multiple ionizable groups can also produce almost linear pH dependencies with slopes less than 1.0 [24, 71]. However, structures at pH 8.3 for the wild-type enzyme complexed with NADH in the open and closed conformations do not show evidence for changes in protonation states of any nearby residues [29]. Deprotonation of phosphate or pyrophosphate could affect the pH dependence, but binding of those anions to horse liver ADH is relatively weak [72], and experiments on another mutated yeast ADH did not show significant differences in pH dependencies with Good’s buffers or the phosphate/pyrophosphate buffers.

It seems possible that the binding of NADH ($1/K_{iq}$ and V_2/K_qE_t) to the T45G enzyme is facilitated when the thiolate of Cys-153 is protonated and a water binds to the catalytic zinc, displacing Glu-67, accompanied by the conformational change. Adding a proton would

electrostatically favor binding of NADH. Removing the hydroxyl group in the T45G enzyme could weaken the interaction of a water bound to the zinc and unmask the participation of Cys-153 in the interchange of zinc ligands. At pH 7, the T45G substitution decreases by ~ 80-fold V_2/K_qE_t, the kinetic constant that includes the isomerization of E-NADH to F-NADH.

4.5. pH dependencies for binding and reactions of substrates

The pH dependencies for V_1/E_t and V_1/K_bE_t for the T45G enzyme are similar, with maximal activities at high pH, above a pK value of 6.3 as compared to values of 7.0 and 7.7 for wild-type enzyme (Table 4). The classical interpretation for the wild-type yeast and horse enzymes is that the zinc ligand (water or alcohol) must be deprotonated for activity, and that His-48 (His-51 in horse ADH1E) in the proton relay system participates as a base that controls the pK value. The H48Q substitution in yeast ADH decreases catalytic efficiencies by ~10-fold, and the pH dependence becomes more complicated, increasing almost linearly (with a log-log slope of ~ 0.54) up to pH 9 with a double wave that could be fitted by pK values of 6.8 and 8.7 [24]. Likewise, the H48E substitution decreases activity by ~100-fold, and activity increases up to pH 10 with pK values of 6.5 and 8.9. (The double wave resembles a “hollow” dependence, which can result when proton transfer is “sticky” and the rate at which the alcohol can deprotonate and transfer a hydride ion from the alkoxide is decreased [50, 51].) The pH dependencies with pK values of 6.8 and 6.5 for these two enzymes with substitutions of His-48 and the pK value of 6.3 for the T45G could all be due to the ionization of the zinc-water or the zinc-alcohol in the complexes with NAD^+, but ionization of His-48 in T45G ADH1 might still contribute because it binds to the nicotinamide ribose (Fig. 1).

Interpreting the pK values for wild-type yeast ADH is not certain because the apparent pK values for V_1/E_t and V_1/K_bE_t can be shifted because of isomerizations in the mechanism. In contrast, the pH dependence of competitive inhibitors should produce “true” values. For wild-type yeast ADH1, the dependence of the negative logarithm of the competitive inhibition constant (log $(1/K_i)$) for trifluoroethanol against ethanol on pH increases essentially linearly from pH 6 to 10 with a slope of + 0.38 [48]. (We confirmed this linear dependence.) The pH dependence reflects the binding to the enzyme-NAD^+ complex. In contrast, horse liver ADH1E shows a pK value of 7.6 for inhibition by trifluoroethanol, and one proton is released per active site on the formation of the complex with NAD^+ and trifluoroethanol [11, 73]. Binding of trifluoroethanol and catalytic efficiency with cyclohexanol for horse ADH1E show similar bell-shaped pH dependencies with pK values of 7.2 and 10.1, attributed to His-51 and Lys-228 in the enzyme-NAD^+ complex [20]. The H51Q substitution in horse ADH1E shifts the pH dependencies for trifluoroethanol binding and catalytic efficiency on ethanol to give maximum values above a pK value of 8.5, consistent with the zinc-water controlling the pK value [14].

Changing the environment of the catalytic zinc in yeast ADH1 also decreases activity. Substitution of Asp-46, which is hydrogen-bonded to His-66 (Fig. 4), with asparagine decreases catalytic efficiency for ethanol oxidation by ~1000-fold and is described by a pK value of ~6.2 [36]. Substitution of Glu-67, which intermittently binds to the zinc [27–

29], with glutamine decreases efficiency by ~100-fold and produces a pH profile with a prominent pK value of ~6.8 and a further increase in activity at higher pH above a pK value of ~9.4. The C153D substitution decreases catalytic efficiency at pH 7.3 by 18-fold for ethanol oxidation and 8-fold for acetaldehyde reduction without greatly affecting the pK values [26]. The D46N, E67Q, and C153D substitutions probably affect the exchange of ligands on the catalytic zinc.

For the T45G enzyme, pH dependencies for V_2/E_t and V_2/K_pE_t are essentially linear, with a modest increase of ~3-fold as pH decreases by 3.4 units. Wild-type enzyme is similar, increasing 3–6-fold as pH decreases, with pK values of 7.0 and 7.8. The H44R ADH has more distinct dependencies, with pK values of 6.6 and 7.6, for the two kinetic constants, respectively [21]. Horse liver ADH shows maximum catalytic efficiency for acetaldehyde reduction below a pK value of 8.6, whereas the H51Q substitution shifts the pK value up to 10, apparently because protonation of the alkoxide through the proton relay system is diminished [14]. It was proposed that a residue with a pK value of 8.25 in wild-type yeast ADH1 was involved as a base in alcohol oxidation and as an acid in aldehyde reduction [15, 18]. The common pK of 7.7 for the pH dependencies of V_1/K_bE_t and V_2/K_pE_t given in Table 4 would be consistent with a histidine residue, but it appears that the reactions of the NADH complexes of the yeast wild-type and T45G enzymes (V_2/E_t and V_2/K_pE_t) are only modulated by protonation of some group(s) in the pH range from 5.5–9.0, which could include His-48.

4.6. Disruption of the proton relay system

The T45G substitution substantially decreases the turnover numbers and catalytic efficiencies for both ethanol oxidation and acetaldehyde reduction and significantly alters the pH dependencies. It appears that the connection of the zinc-bound water to the solvent in the proton relay is disrupted when the Thr-45 hydroxyl group is deleted.

Previous studies on the yeast enzyme with the T45A and T45C substitutions suggested that these enzymes had turnover numbers for ethanol oxidation that were less than $1/10^4$ that of wild-type enzyme [24]. The T45G enzyme has a turnover number in the standard assay of 0.18 s^{-1}, and the value estimated for the T45A enzyme is 0.016 s^{-1}, which suggests that a water as shown in Fig. 1 does not fully replace the catalytic contribution of the Thr-45 hydroxyl group [70]. Structural modeling shows close contacts of such a water with atoms in the active site (e.g., 2.4 Å to Gly-45 CA), and it appears that a productive position would be sterically hindered in ternary complexes with an alcohol or aldehyde. The T45G substitution decreases binding of trifluoroethanol by only 10-fold, but some steric conflicts could have significant effects on transition states and rates of proton and hydride transfer.

The T45C yeast ADH might have been expected to retain activity if the cysteine residue could participate in the hydrogen bond system. However, the conversion of the active site serine in subtilisin to a cysteine, by a “chemical mutation” based on research by Henry Weiner, made an enzyme that had < 1/100 of the activity of wild-type enzyme on peptide substrates [74, 75]. Apparently the slightly larger size or deficiency of hydrogen bonding of the sulfur as compared to an oxygen severely impacts proton transfer.

The homologous S48A substitution in the horse liver ADH1E decreases turnover with ethanol by 200-fold, to 0.018 s^{-1}, affinity for NAD^+ by 4-fold, and catalytic efficiency for ethanol oxidation by 7×10^5-fold [6]. The T48A substitution also inactivates human ADH1B [76]. These results show that conservative substitutions (glycine, alanine or cysteine) of the serine or threonine residues substantially decrease catalytic activity of ADHs, probably by disrupting the proton relay system.

Benzyl alcohol is oxidized by yeast ADH1 with a turnover number of 0.012 s^{-1} and ADH2 with a value of 1.9 s^{-1} [77]. Deuterium isotope effects on turnover numbers ($^D V/E_t$ = 3.6–4.1) show that hydride transfer is at least partly rate-limiting step in the oxidation of 4-methylbenzyl alcohol and the reduction of 4-methylbenzaldehyde [18]. The lower activity on these large aromatic substrates as compared to ethanol is probably because of steric hindrance and poor productive binding [77], which also would occur with the T45G enzyme acting on ethanol.

The T45G substitution did not change an ionizable amino acid, but does alter the rate constants and pH dependencies, exposing a modest pH dependence for V_1/E_t and V_1/K_bE_t with a pK value of 6.3. Likewise, the H44R, D46N, H48Q, H48E, and E67Q substitutions all decreased catalytic efficiency for ethanol oxidation (V_1/K_bE_t) and exposed pH dependencies with pK values of 6.1–6.8, as compared to the pK value of 7.7 for wild-type enzyme [24]. Thus, it is tempting to assign the pK value of 6.3 for the T45G enzyme to the ionization of the zinc-water in the enzyme-NAD^+ complex. However, the pH dependencies for the H48Q and H48E enzymes can be described by two ionizable groups with the second pK value in the range of 8.7–10, and thus it is possible that the higher pK value is due to the zinc-water. Dependencies of kinetic constants on pH are complex functions of the contributions of each amino acid residue to the microscopic rate constants in the enzyme mechanism, and it is difficult to assign a specific role for a particular amino acid [71].

The role of His-48 in catalysis needs further study. Analysis of Fig. 1 shows that the proton relay would require a small, but energetically feasible rotation of single bonds of His-48 to move the imidazole group so that NE2 accepts a hydrogen bond from the 2'-hydroxyl group of the nicotinamide ribose rather than from the 3'-hydroxyl group. This movement would disrupt the hydrogen bond from ND1 to Asp-53, but after the proton is relayed from the zinc ligand to the imidazole (Scheme 1), Asp-53 could stabilize the protonated imidazole or facilitate the transfer to bulk solvent. His-51 contributes to catalysis in liver ADHs, but substitutions with glutamine do not completely abolish activity [14, 24, 78]. Proton and hydride transfers in ADHs deserve further computational studies of the dynamics [79–81].

The T45G substitution changes the pH dependencies for binding of NADH and catalytic efficiencies and disrupts the proton relay to His-48, but the mechanism of proton transfer is not clear in this new enzyme. A water molecule can bind to the zinc in the enzyme-coenzyme complexes and allow the coordination of the catalytic zinc to change and substrates to bind, but it appears that a water would not easily replace the hydroxyl group of Thr-48 and fit well in the proton relay system. Perhaps a transient pentacoordinate species with a water and the oxygen of a substrate forms with the zinc and slowly transfers the

proton. Perhaps the thiol/thiolate group of Cys-153 participates, or conformational states might be altered. It is clear that the serine or threonine residues in the yeast and liver ADHs have a critical role in catalysis.

Acknowledgments

This work was supported by USPHS National Institute on Alcohol Abuse and Alcoholism grant AA00279 and National Science Foundation grant MCB 9118657. We thank E. T. Young and B. D. Hall for the ADH-negative yeast strain and the plasmid with the ADH gene and Darla Ann Kratzer and Edda Warth for the sequencing the complete gene. We dedicate this work to Hans Eklund for his leadership in structural studies of alcohol dehydrogenases.

Abbreviations:

ADH	alcohol dehydrogenase
T45G	substitution of Thr-45 with Gly-45

References

[1]. Brändén C-I, Jörnvall H, Eklund H, Furugren B, Alcohol Dehydrogenases, The Enzymes, 3rd Ed. 11 (1975) 103–190.

[2]. Eklund H, Nordström B, Zeppezauer E, Söderlund G, Ohlsson I, Boiwe T, Söderberg BO, Tapia O, Brändén C-I, Åkeson Å, Three-dimensional structure of horse liver alcohol dehydrogenase at 2.4 Å resolution, J. Mol. Biol 102 (1976) 27–59. [PubMed: 178875]

[3]. Eklund H, Plapp BV, Samama JP, Brändén C-I, Binding of substrate in a ternary complex of horse liver alcohol dehydrogenase, J. Biol. Chem 257 (1982) 14349–14358. [PubMed: 6754727]

[4]. Sekhar VC, Plapp BV, Rate constants for a mechanism including intermediates in the interconversion of ternary complexes by horse liver alcohol dehydrogenase, Biochemistry 29 (1990) 4289–4295. [PubMed: 2161681]

[5]. Plapp BV, Ramaswamy S, Atomic-resolution structures of horse liver alcohol dehydrogenase with NAD^+ and fluoroalcohols define strained Michaelis complexes, Biochemistry 51 (2012) 4035–4048. [PubMed: 22531044]

[6]. Kim K, Plapp BV, Inversion of substrate specificity of horse liver alcohol dehydrogenase by substitutions of Ser-48 and Phe-93, Chem.-Biol. Interact 276 (2017) 77–87. [PubMed: 28025168]

[7]. Kim K, Plapp BV, Substitutions of amino acid residues in the substrate binding site of horse liver alcohol dehydrogenase have small effects on the structures but significantly affect catalysis of hydrogen transfer, Biochemistry 59 (2020) 862–879. [PubMed: 31994873]

[8]. Dalziel K, Kinetic studies of liver alcohol dehydrogenase and pH effects with coenzyme preparations of high purity, J. Biol. Chem 238 (1963) 2850–2858. [PubMed: 14063314]

[9]. Brooks RL, Shore JD, Gutfreund H, The effects of pH and temperature on hydrogen transfer in the liver alcohol dehydrogenase mechanism, J. Biol. Chem 247 (1972) 2382–2383. [PubMed: 4336373]

[10]. Kvassman J, Pettersson G, Unified mechanism for proton-transfer reactions affecting the catalytic activity of liver alcohol dehydrogenase, Eur. J. Biochem 103 (1980) 565–575. [PubMed: 6987061]

[11]. Kovaleva EG, Plapp BV, Deprotonation of the horse liver alcohol dehydrogenase-NAD^+ complex controls formation of the ternary complexes, Biochemistry 44 (2005) 12797–12808. [PubMed: 16171395]

[12]. Plapp BV, Savarimuthu BR, Ferraro DJ, Rubach JK, Brown EN, Ramaswamy S, Horse liver alcohol dehydrogenase: zinc coordination and catalysis, Biochemistry 56 (2017) 3632–3646. [PubMed: 28640600]

[13]. LeBrun LA, Plapp BV, Control of coenzyme binding to horse liver alcohol dehydrogenase, Biochemistry 38 (1999) 12387–12393. [PubMed: 10493806]

[14]. LeBrun LA, Park DH, Ramaswamy S, Plapp BV, Participation of histidine-51 in catalysis by horse liver alcohol dehydrogenase, Biochemistry 43 (2004) 3014–3026. [PubMed: 15023053]

[15]. Dickenson CJ, Dickinson FM, A study of the pH- and temperature-dependence of the reactions of yeast alcohol dehydrogenase with ethanol, acetaldehyde and butyraldehyde as substrates, Biochem. J 147 (1975) 303–311. [PubMed: 241323]

[16]. Dickenson CJ, Dickinson FM, A study of the oxidation of butan-1-ol and propan-2-ol by nicotinamide-adenine dinucleotide catalysed by yeast alcohol dehydrogenase, Biochem. J 147 (1975) 541–547. [PubMed: 170911]

[17]. Dickenson CJ, Dickinson FM, A study of the ionic properties of the essential histidine residue of yeast alcohol dehydrogenase in complexes of the enzyme with its coenzymes and substrates, Biochem. J, 161 (1977) 73–82. [PubMed: 15541]

[18]. Klinman JP, Acid-base catalysis in the yeast alcohol dehydrogenase reaction, J. Biol. Chem 250 (1975) 2569–2573. [PubMed: 235517]

[19]. Cook PF, Cleland WW, pH variation of isotope effects in enzyme-catalyzed reactions. 1. Isotope- and pH-dependent steps the same, Biochemistry 20 (1981) 1797–1805. [PubMed: 7013800]

[20]. Cook PF, Cleland WW, pH variation of isotope effects in enzyme-catalyzed reactions. 2. Isotope-dependent step not pH dependent. Kinetic mechanism of alcohol dehydrogenase, Biochemistry 20 (1981) 1805–1816. [PubMed: 7013801]

[21]. Gould RM, Plapp BV, Substitution of arginine for histidine-47 in the coenzyme binding site of yeast alcohol dehydrogenase I, Biochemistry 29 (1990) 5463–5468. [PubMed: 2201405]

[22]. Hennecke M, Plapp BV, Involvement of histidine residues in the activity of horse liver alcohol dehydrogenase, Biochemistry 22 (1983) 3721–3728. [PubMed: 6351909]

[23]. Plapp BV, Ganzhorn AJ, Gould RM, Green DW, Hershey AD, Structure and function in yeast alcohol dehydrogenases, Prog. Clin. Biol. Res 232 (1987) 227–236. [PubMed: 3303037]

[24]. Plapp BV, Ganzhorn AJ, Gould RM, Green DW, Jacobi T, Warth E, Kratzer DA, Catalysis by yeast alcohol dehydrogenase, Adv. Exp. Med. Biol 284 (1991) 241–251. [PubMed: 2053479]

[25]. Sun HW, Plapp BV, Progressive sequence alignment and molecular evolution of the Zn-containing alcohol-dehydrogenase family, J. Mol. Evol 34 (1992) 522–535. [PubMed: 1593644]

[26]. Kim K, Plapp BV, Substitution of cysteine-153 ligated to the catalytic zinc in yeast alcohol dehydrogenase with aspartic acid and analysis of mechanisms of related medium chain dehydrogenases, Chem.-Biol. Interact 302 (2019) 172–182. [PubMed: 30721696]

[27]. Savarimuthu BR, Ramaswamy S, Plapp BV, Yeast alcohol dehydrogenase structure and catalysis, Biochemistry 53 (2014) 5791–5803. [PubMed: 25157460]

[28]. Plapp BV, Charlier HA Jr., Ramaswamy S, Mechanistic implications from structures of yeast alcohol dehydrogenase complexed with coenzyme and an alcohol, Arch. Biochem. Biophys 591 (2016) 35–42. [PubMed: 26743849]

[29]. Guntupalli SR, Zhuang L, Chang L, Plapp BV, Subramanian R, Cryo-electron microscopy structures of yeast alcohol dehydogenase, Biochemistry 60 (2021) 663–677. [PubMed: 33620215]

[30]. Green DW, Sun HW, Plapp BV, Inversion of the substrate specificity of yeast alcohol dehydrogenase, J. Biol. Chem 268 (1993) 7792–7798. [PubMed: 8463307]

[31]. Harris M, Jones TA, Molray - a web interface between O and the POV-Ray ray tracer, Acta Crystallogr. D57 (2001) 1201–1203.

[32]. Bennetzen JL, Hall BD, The primary structure of the *Saccharomyces cerevisiae* gene for alcohol dehydrogenase, J. Biol. Chem 257 (1982) 3018–3025. [PubMed: 6277922]

[33]. Broach JR, Strathern JN, Hicks JB, Transformation in yeast: Development of a hybrid cloning vector and isolation of the *CAN1* gene, Gene 8 (1979) 121–133. [PubMed: 395029]

[34]. Kunkel TA, Roberts JD, Zakour RA, Rapid and efficient site-specific mutagenesis without phenotypic selection, Methods Enzymol. 154 (1987) 367–382. [PubMed: 3323813]

[35]. Zoller MJ, Smith M, Oligonucleotide-directed mutagenesis: a simple method using two oligonucleotide primers and a single-stranded DNA template, DNA 3 (1984) 479–488. [PubMed: 6096101]

[36]. Ganzhorn AJ, Plapp BV, Carboxyl groups near the active site zinc contribute to catalysis in yeast alcohol dehydrogenase, J. Biol. Chem 263 (1988) 5446–5454. [PubMed: 3281940]

[37]. Sanger F, Nicklen S, Coulson AR, DNA sequencing with chain-terminating inhibitors, Proc. Natl. Acad. Sci. U.S.A 74 (1977) 5463–5467. [PubMed: 271968]

[38]. Young ET, Pilgrim D, Isolation and DNA sequence of ADH3, a nuclear gene encoding the mitochondrial isozyme of alcohol dehydrogenase in *Saccharomyces cerevisiae* Mol. Cell. Biol 5 (1985) 3024–3034.

[39]. Ganzhorn AJ, Green DW, Hershey AD, Gould RM, Plapp BV, Kinetic characterization of yeast alcohol dehydrogenases. Amino acid residue 294 and substrate specificity, J. Biol. Chem 262 (1987) 3754–3761. [PubMed: 3546317]

[40]. Theorell H, Yonetani T, Liver alcohol dehydrogenase-DPN-pyrazole complex: A model of a ternary intermediate in the enzyme reaction, Biochem. Z 338 (1963) 537–553. [PubMed: 14087322]

[41]. Plapp BV, Enhancement of the activity of horse liver alcohol dehydrogenase by modification of amino groups at the active sites, J. Biol. Chem 245 (1970) 1727–1735. [PubMed: 4314596]

[42]. Cornell NW, Properties of alcohol dehydrogenase and ethanol oxidation *in vivo* and in hepatocytes, Pharmacol. Biochem. Behav 18 Suppl 1 (1983) 215–221. [PubMed: 6356160]

[43]. Cleland WW, Statistical analysis of enzyme kinetic data, Methods Enzymol. 63 (1979) 103–138. [PubMed: 502857]

[44]. Rubach JK, Plapp BV, Amino acid residues in the nicotinamide binding site contribute to catalysis by horse liver alcohol dehydrogenase, Biochemistry 42 (2003) 2907–2915. [PubMed: 12627956]

[45]. Bäcklin KI, The equilibrium constant of the system ethanol, aldehyde, DPN^+, DPNH and H^+, Acta Chem. Scand 12 (1958) 1279–1285.

[46]. Wratten CC, Cleland WW, Product inhibition studies on yeast and liver alcohol dehydrogenases, Biochemistry 2 (1963) 935–941. [PubMed: 14087384]

[47]. Dickinson FM, Monger GP, A study of the kinetics and mechanism of yeast alcohol dehydrogenase with a variety of substrates, Biochem. J 131 (1973) 261–270. [PubMed: 4352908]

[48]. Dickenson CJ, Dickinson FM, Inhibition by ethanol, acetaldehyde and trifluoroethanol of reactions catalysed by yeast and horse liver alcohol dehydrogenases, Biochem. J 171 (1978) 613–627. [PubMed: 208509]

[49]. Northrop DB, Deuterium and tritium kinetic isotope effects on initial rates, Methods Enzymol. 87 (1982) 607–625. [PubMed: 7176927]

[50]. Cleland WW, The use of pH studies to determine chemical mechanisms of enzyme-catalyzed reactions, Methods Enzymol. 87 (1982) 390–405. [PubMed: 7176923]

[51]. Cook PF, Cleland WW, Enzyme Kinetics and Mechanism, Taylor & Francis Group, LLC., New York, 2007.

[52]. Dworschack RT, Plapp BV, Kinetics of native and activated isozymes of horse liver alcohol dehydrogenase, Biochemistry 16 (1977) 111–116. [PubMed: 831772]

[53]. Fan F, Plapp BV, Substitutions of isoleucine residues at the adenine binding site activate horse liver alcohol dehydrogenase, Biochemistry 34 (1995) 4709–4713. [PubMed: 7718576]

[54]. Plapp BV, Lee AT, Khanna A, Pryor JM, Bradykinetic alcohol dehydrogenases make yeast fitter for growth in the presence of allyl alcohol, Chem.-Biol. Interact 202 (2013) 104–110. [PubMed: 23200945]

[55]. Pahari S, Sun L, Alexov E, PKAD: a database of experimentally measured pKa values of ionizable groups in proteins, Database 2019 (2019) 1–7.

[56]. Klinman JP, Welsh K, The zinc content of yeast alcohol dehydrogenase, Biochem. Biophys. Res. Commun 70 (1976) 878–884. [PubMed: 779786]

[57]. Sytkowski AJ, Metal stoichiometry, coenzyme binding, and zinc and cobalt enchange in highly purified yeast alcohol dehydrogenase, Arch. Biochem. Biophys 184 (1977) 505–517. [PubMed: 202199]

[58]. Maret W, Andersson I, Dietrich H, Schneider Bernlöhr H, Einarsson R, Zeppezauer M, Site-specific substituted cobalt(II) horse liver alcohol dehydrogenases. Preparation and

characterization in solution, crystalline and immobilized state, Eur. J. Biochem 98 (1979) 501–512. [PubMed: 488110]

[59]. Sytkowski AJ, Vallee BL, Cobalt exchange in horse liver alcohol dehydrogenase, Biochemistry 17 (1978) 2850–2857. [PubMed: 210784]

[60]. Kvassman J, Pettersson G, Effect of pH on coenzyme binding to liver alcohol dehydrogenase, Eur. J. Biochem 100 (1979) 115–123. [PubMed: 39751]

[61]. Pettersson G, Liver alcohol dehydrogenase, CRC Crit. Rev. Biochem 21 (1987) 349–389. [PubMed: 3304836]

[62]. Sekhar VC, Plapp BV, Mechanism of binding of horse liver alcohol dehydrogenase and nicotinamide adenine dinucleotide, Biochemistry 27 (1988) 5082–5088. [PubMed: 3167032]

[63]. Andersson P, Kvassman J, Lindström A, Oldén B, Pettersson G, Effect of NADH on the pKa of zinc-bound water in liver alcohol dehydrogenase, Eur. J. Biochem 113 (1981) 425–433. [PubMed: 7011796]

[64]. DeTraglia MC, Schmidt J, Dunn MF, McFarland JT, Liver alcohol dehydrogenase-coenzyme reaction rates, J. Biol. Chem 252 (1977) 3493–3500. [PubMed: 16905]

[65]. Andersson P, Kvassman J, Oldén B, Pettersson G, Electrostatic field effects of coenzymes on ligand binding to catalytic zinc in liver alcohol dehydrogenase, Eur. J. Biochem 138 (1984) 603–609. [PubMed: 6363076]

[66]. Pettersson G, Eklund H, Electrostatic effects of bound NADH and NAD^+ on ionizing groups in liver alcohol dehydrogenase, Eur. J. Biochem 165 (1987) 157–161. [PubMed: 3569292]

[67]. Fan F, Plapp BV, Probing the affinity and specificity of yeast alcohol dehydrogenase I for coenzymes, Arch. Biochem. Biophys 367 (1999) 240–249. [PubMed: 10395740]

[68]. Ryde U, On the role of Glu-68 in alcohol dehydrogenase, Protein Sci. 4 (1995) 1124–1132. [PubMed: 7549877]

[69]. Sanghani PC, Robinson H, Bosron WF, Hurley TD, Human glutathione-dependent formaldehyde dehydrogenase. Structures of apo, binary, and inhibitory ternary complexes, Biochemistry 41 (2002) 10778–10786. [PubMed: 12196016]

[70]. Gould RM, Histidines in the Mechanism of Yeast Alcohol Dehydrogenase, Ph. D. Thesis, Biochemistry, The University of Iowa, 1988.

[71]. Plapp BV, Site-directed mutagenesis: a tool for studying enzyme catalysis, Methods Enzymol. 249 (1995) 91–119. [PubMed: 7791629]

[72]. Oldén B, Pettersson G, Anion binding to liver alcohol dehydrogenase, Eur. J. Biochem 125 (1982) 311–315. [PubMed: 6749494]

[73]. Shore JD, Gutfreund H, Brooks RL, Santiago D, Santiago P, Proton equilibria and kinetics in the liver alcohol dehydrogenase reaction mechanism, Biochemistry 13 (1974) 4185–4191. [PubMed: 4370301]

[74]. Weiner H, White WN, Hoare DG, Koshland DE Jr., The formation of anhydrochymotrypsin by removing the elements of water from the serine at the active site, J. Am. Chem. Soc 88 (1966) 3851–3859. [PubMed: 5916376]

[75]. Neet KE, Koshland DE Jr., The conversion of serine at the active site of subtilisin to cysteine: a “chemical mutation”, Proc. Natl. Acad. Sci. U.S.A 56 (1966) 1606–1611. [PubMed: 5230319]

[76]. Höög J-O, Eklund H, Jörnvall H, A single-residue exchange gives human recombinant ββ alcohol dehydrogenase γγ isozyme properties, Eur. J. Biochem 205 (1992) 519–526. [PubMed: 1572355]

[77]. Pal S, Park DH, Plapp BV, Activity of yeast alcohol dehydrogenases on benzyl alcohols and benzaldehydes. Characterization of ADH1 from *Saccharomyces carlsbergensis* and transition state analysis, Chem.-Biol. Interact 178 (2009) 16–23. [PubMed: 19022233]

[78]. Ehrig T, Hurley TD, Edenberg HJ, Bosron WF, General base catalysis in a glutamine for histidine mutant at position 51 of human liver alcohol dehydrogenase, Biochemistry 30 (1991) 1062–1068. [PubMed: 1989677]

[79]. Agarwal PK, Webb SP, Hammes-Schiffer S, Computational studies of the mechanism for proton and hydride transfer in liver alcohol dehydrogenase, J. Am. Chem. Soc 122 (2000) 4803–4812.

[80]. Luo J, Bruice TC, Dynamic structures of horse liver alcohol dehydrogenase (HLADH): Results of molecular dynamics simulations of HLADH-NAD^+-$PhCH_2OH$, HLADH-NAD^+-$PhCH_2O^-$, and HLADH-NADH-PhCHO, J. Am. Chem. Soc 123 (2001) 11952–11959. [PubMed: 11724603]

[81]. Cui Q, Elstner M, Karplus M, A theoretical analysis of the proton and hydride transfer in liver alcohol dehydrogenase (LADH). J. Phys. Chem. B 106 (2002) 2721–2740.

Highlights

- Threonine 45 is a critical amino acid in catalysis by yeast ADH.
- The Thr45Gly substitution disrupts the proton relay system.
- The pH dependencies for catalysis by yeast and liver ADHs are compared.
- The inverted coordination of zinc in the yeast apoenzyme affects NAD binding.
- Binding of NADH to the Thr45Gly ADH is linearly dependent on pH.

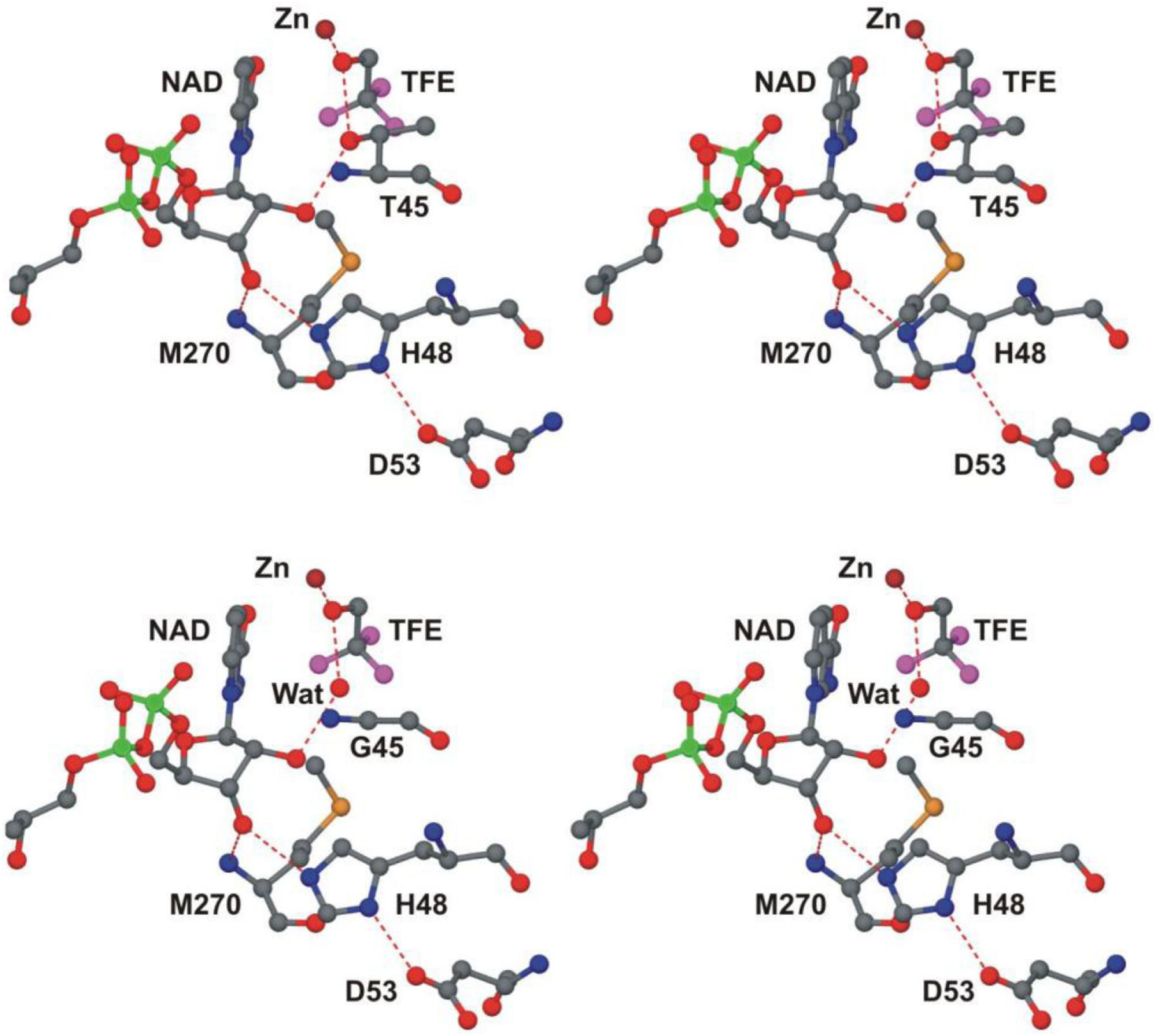

Fig. 1.

Structural models of the proton relay system in yeast ADH1. Top figure shows the structure of the complex with NAD^+ and trifluoroethanol (TFE) determined by X-ray crystallography at 2.4 Å (4W6Z.pdb, subunit A). The bottom figure shows how a water might replace the hydroxyl group of Thr-45 in the T45G enzyme and facilitate the connection between the alcohol and the solvent. The figure was prepared with the Molray interface server in Uppsala [31]. Atoms are color coded: oxygen (red), carbon (gray), nitrogen (blue), phosphorus (green), zinc (brown), fluorine (magenta). The dashed red lines represent hydrogen bonds.

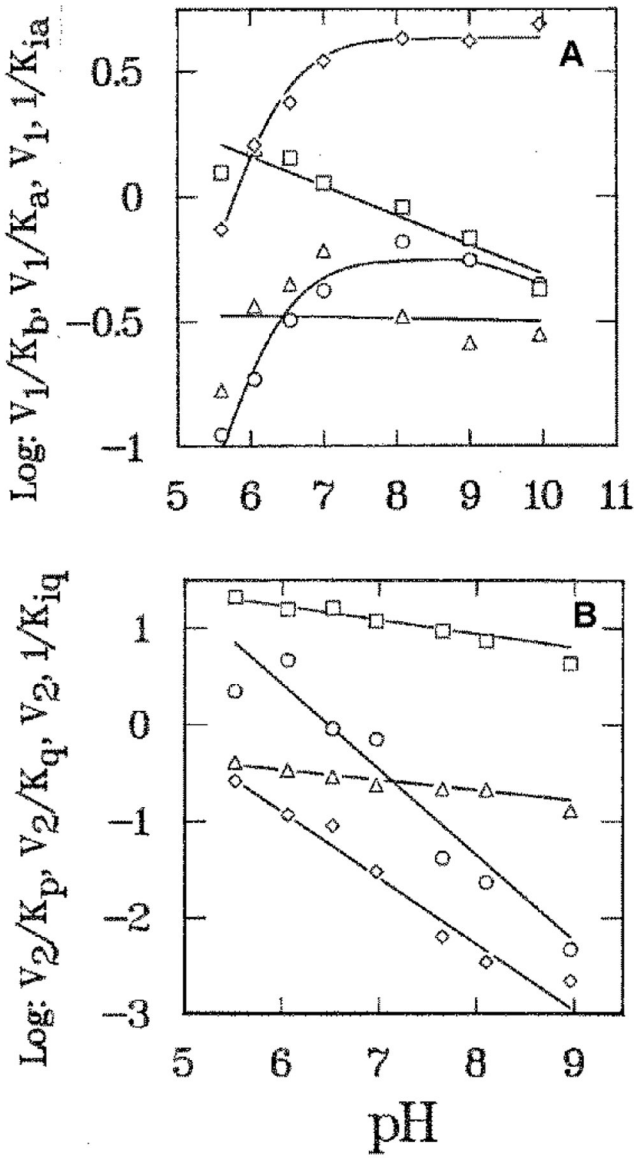

Fig. 2.

pH dependencies for the kinetic constants of the T45G enzyme. The logarithms of the kinetic constants are plotted, and the units (chosen to put values on the same graph) for each parameter are defined with the symbols below. The lines are calculated from the fits to the equations given in Table 4. (A) Forward reaction: V_1/E_t (s^{-1}1 ○), V_1/K_bE_t ($M^{-1}s^{-1}$ ◊), $1/K_{ia}$ (mM^{-1} □), V_1/K_aE_t, ($mM^{-1}s^{-1}$ Δ). The fitted line for Log V_1/E_t shows the fit to a bell-shaped pH dependence, but the estimated value for upper pK was uncertain at 10.5 ± 0.4, and the fit to Eq. 1 in Table 4 was better. (B) Reverse reaction: V_2/E_t (s^{-1} □), V_2/K_pE_t (mM^{-1} s^{-1} Δ), V_2/K_qE_t ($\mu M^{-1}s^{-1}$ ○), $1/K_{iq}$, (μM^{-1} ◊).

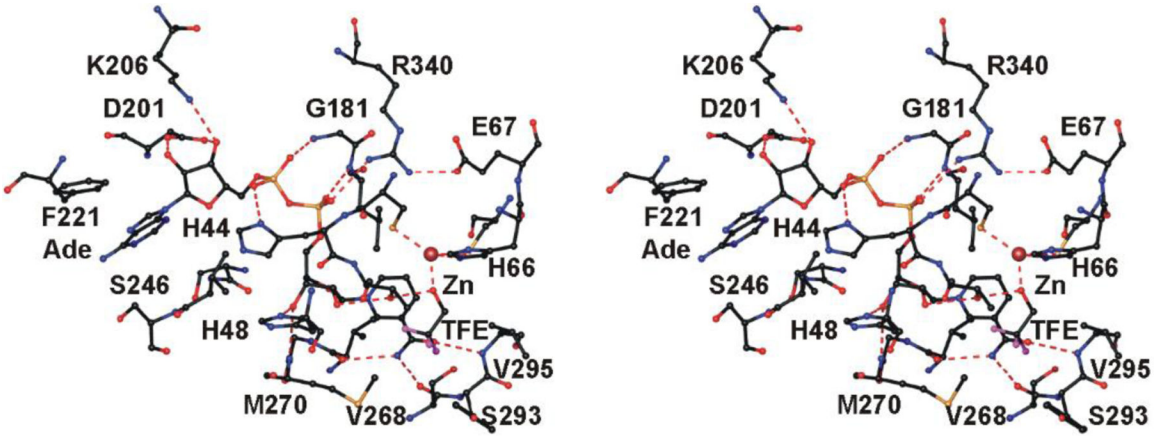

Fig. 3.

Active site of the wild-type yeast enzyme, showing interactions of amino acid residues with the coenzyme (Ade for adenine ring), catalytic zinc and trifluoroethanol (TFE). This is the closed conformation based on subunit A from 5ENV.pdb [28]. Atom colors are described in Fig. 1, except phosphorus is gold here. The dashed red lines represent hydrogen bonds. Views of the open and closed conformations and the different coordinations of the catalytic zinc are shown in Refs. [28, 29].

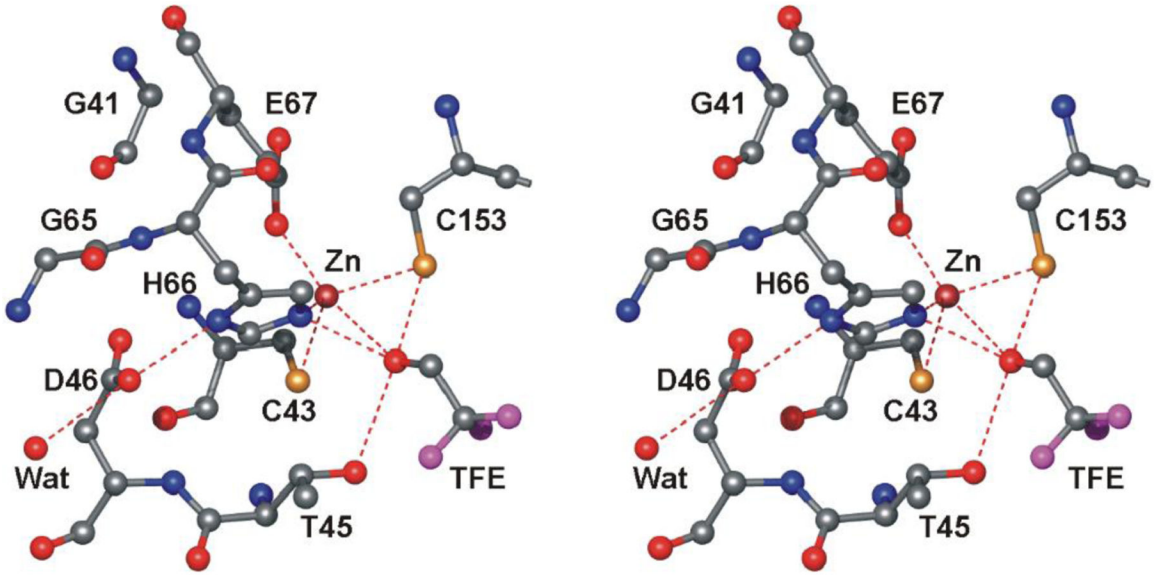

Fig. 4.

Interactions of ligands to the catalytic zinc in the open enzyme conformation showing a potential trigonal bipyramidal, pentacoordinate intermediate in the interchange of ligands. The red dashes indicate zinc coordination and hydrogen bonds where the distances (Å) to the zinc differ in the open versus (closed) conformations: His-66 NE2 2.2 (2.1), Cys-43 SG 2.4 (2.3), Cys-153 SG 2.5 (2.4), TFE O 3.0 (1.9), Glu-67 OE2 2.3 (4.9). The model is based on subunits B and D (4W6Z.pdb [27]), which have no coenzyme bound, and is similar to subunit B (5ENV.pdb [28]), which has bound NAD^+. The crystals were prepared in the presence of 0.1–0.5 M 2,2,2-trifluoroethanol (TFE) and ~ 2 mM NAD^+, but crystal lattice contacts apparently prevent the conformational change [29].

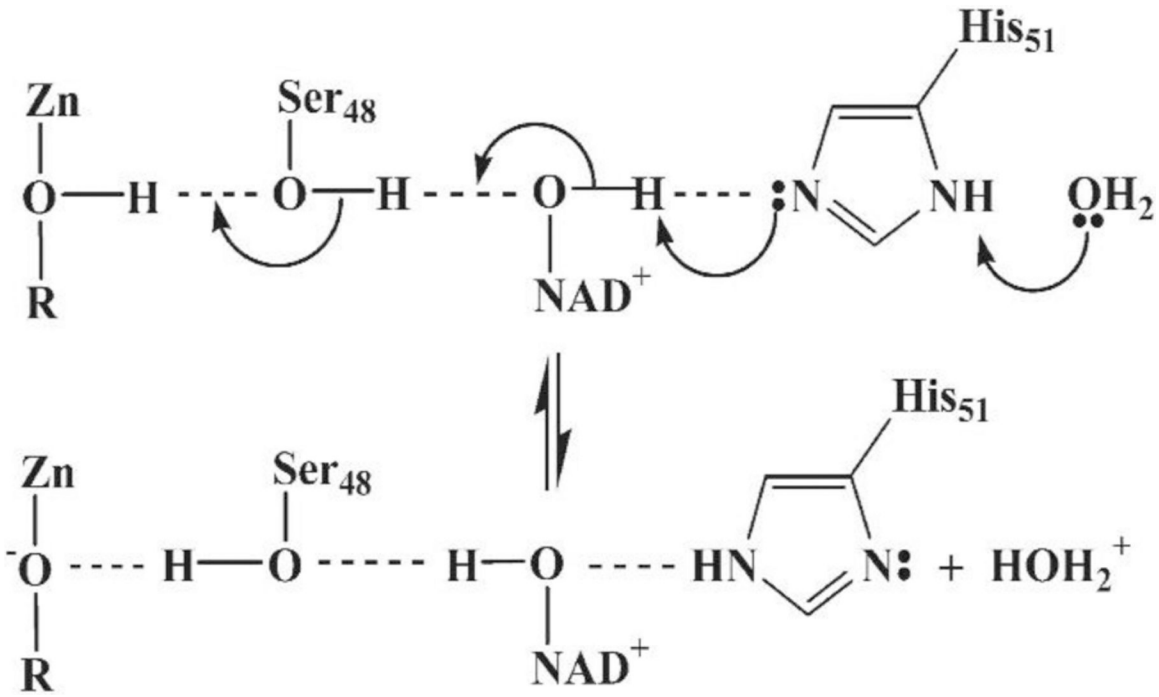

Scheme 1.
Proton Relay System in Horse Liver ADH

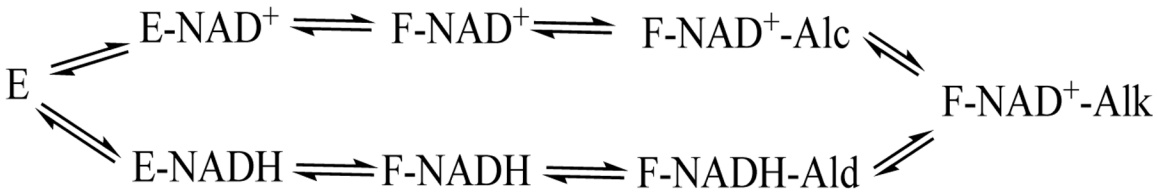

Scheme 2.
General Mechanism for Alcohol Dehydrogenases

Table 1

Kinetic constants for wild-type and T45G yeast alcohol dehydrogenases.[a]

Constant	wild type[b]	T45G
K_a (μM), NAD^+	160	1500
K_b (mM), ethanol	21	130
K_p (mM), acetaldehyde	0.74	32
K_q (μM), NADH	94	47
K_{ia} (μM), NAD^+	950	1600
K_{iq} (μM), NADH	31	70
V_1/E_t (s^{-1})	360	0.64
V_2/E_t (s^{-1})	1800	7.8
K_i (mM), CF_3CH_2OH	2.5	27
Activity (s^{-1})	400	0.18
K_{eq} (pM)	12	42

[a] K_a, K_b, K_p, and K_q are the Michaelis constants for NAD^+, ethanol, NADH and acetaldehyde respectively. K_i values are the dissociation (inhibition) constants. V_1/E_t is the turnover number for ethanol oxidation and V_2/E_t is the turnover number for acetaldehyde reduction, where E_t is the concentration of subunits ("active" sites). The buffer was 83 mM potassium phosphate with 40 mM KCl and 0.25 mM EDTA at pH 7.3 and 30 °C. "Activity" is the turnover number in the standard assay [41] at 30 °C, based on titration of the active sites. The equilibrium constant is calculated from the Haldane equation, $K_{eq} = V_1 K_p K_{iq}[H^+]/V_2 K_b K_{ia}$, where $[H^+] = 5 \times 10^{-8}$ M at pH 7.3. The experimental value is 10 pM [45].

[b] From Ref. [21].

Table 2

Deuterium isotope effects for oxidation of ethanol.[a]

Enzyme/KIE	$^{D}V_1/E_t$	$^{D}V_1/K_bE_t$	$^{D}V_1/K_aE_t$	$^{D}(1/K_{ia})$
T45G	3.9 ± 0.2	3.6 ± 0.3	2.5 ± 0.2	1.1 ± 0.2
wild-type[b]	1.2 ± 0.2	2.0 ± 0.4	1.8 ± 0.2	1.0 ± 0.2

[a] Nomenclature of Northrop [49]. Determined by initial velocity studies with co-varied coenzyme and substrate with 17-fold range of concentrations in a 5 × 5 matrix with duplicate assays.

[b] Somewhat higher values are reported in Ref. [36].

Table 3

Dependencies of kinetic constants on pH for T45G yeast alcohol dehydrogenase.[a]

Constant / pH	5.60	6.05	6.54	7.00	–	8.07	9.00	9.95
K_a (μM), NAD^+	660	510	720	690	–	2100	2140	1580
K_b (mM), CH_3CH_2OH	150	116	135	120	–	190	130	91
K_{ia} (μM), NAD^+	800	650	720	880	–	1130	1470	2370
V_1/E_t (s^{-1})	0.11	0.19	0.32	0.42	–	0.72	0.56	0.44
Constant / pH	5.52	6.06	6.52	7.00	7.65	8.08	8.96	–
K_q (μM), NADH	9.6	3.4	18	13	220	320	910	-
K_p (mM), CH_3CHO	52	46	56	41	43	35	33	–
K_{iq} (μM), NADH	3.8	8.6	11	38	156	290	450	–
V_2/E_t (s^{-1})	21	16	16	9.5	9.3	7.3	4.2	–
K_{eq} (pM)	23	50	37	65		40	10	–

[a]Kinetic constants determined by initial velocity studies with 17-fold varied substrate concentrations in a 5 × 5 matrix with duplicate assays. Standard errors of the fits to Eq. 1 are typically less than 15 %.

Table 4

Apparent macroscopic pK values and kinetic constants at pH limits.[a]

	Wild-type ADH[b]				T45G ADH		
Kinetic constant	**Eq**	**pK**	**Limiting Values**		**Eq**	**pK or log-pH slope**	**Value at high pH or at pH 7**
V_1/E_t (s^{-1})	1	7.0 ± 0.1	k_a	250	2	6.2 ± 0.1	0.52 ± 0.04
			k_b	500			
V_1/K_bE_t (M^{-1} s^{-1})	1	7.7 ± 0.1	k_a	3200	2	6.30 ± 0.05	4.3 ± 0.2
			k_b	25000			
$1/K_{ia}$ (mM^{-1})[b]	1	8.1 ± 0.2	k_a	1.8	4	m − 0.12 ± 0.02	1.1
			k_b	0.20			
V_2/E_t (s^{-1})	1	7.0 ± 0.3	k_a	4000	4	m − 0.14 ± 0.02	12
			k_b	1300			
V_2/K_pE_t (mM^{-1} s^{-1})	1	7.8 ± 0.2	k_a	2900	4	m − 0.11 ± 0.01	0.27
			k_b	450			
V_2/K_qE_t (μM^{-1} s^{-1})	3	7.8 ± 0.1	k_a	32	4	m − 0.89 ± 0.22	0.39
$1/K_{iq}$ (mM^{-1})[b]	1	7.4 ± 0.2	k_a	68	4	m − 0.69 ± 0.09	32
			k_b	2.4			

[a] Data were fitted to the logarithmic forms of the pH dependencies. Eq. 1 is $k_{obs} = (k_a + k_bK_1/[H^+])/(1 + K_1/[H^+])$, where the enzyme reacts in a protonated form that is described by kinetic constant k_a and an unprotonated form (related by K_1) with kinetic constant k_b. When only one form of enzyme is active, the simpler equations apply: Eq. 2, $k_{obs} = k_b/(1 + [H^+]/K_1)$; Eq. 3, $k_{obs} = k_a/(1 + K_1[H^+])$, and Eq. 4 is $k_{obs} = m\,[H^+]$ + intercept.

[b] Data from Ref. [21]. The data for K_{ia} and K_{iq} have been refitted as $1/K_{ia}$ and $1/K_{iq}$, yielding the binding constant and the pK_1 for the free enzyme.